Malaysian Journal of Analytical Sciences (MJAS)



Published by Malaysian Analytical Sciences Society

MOLECULARLY IMPRINTED POLYMERS FOR DOMOIC ACID DETECTION IN SELECTED SHELLFISH TISSUE

(Polimer Tercetak Molekul bagi Pengesanan Domoik Asid di dalam Tisu Kerangan Terpilih)

Fatin Nabilah Muhamad, Hafiza Mohamed Zuki*, Marinah Ariffin, and Azrilawani Ahmad

Faculty of Science and Marine Environment, Universiti Malaysia Terengganu, 21030 Kuala Terengganu, Malaysia

*Corresponding author: hafiza@umt.edu.my

Received: 22 September 2022; Accepted: 27 February 2023; Published: 19 April 2023

Abstract

Domoic acid (DA) molecular imprinted polymers (MIP) were successfully synthesized by a bulk polymerization method using 2-hydroxyethyl methacrylate (HEMA) as a functional monomer and ethylene-glycol dimethacrylate (EGDMA) as a cross-linker. Non-imprinted polymers (NIP) were also synthesized using similar procedures, but without the addition of template molecules (DA). The presence of DA templates in MIP and the absence of DA templates in NIP was proven by Fourier-Transform Infrared (FT-IR) Spectroscopy, Brunauer, Emmett, and Teller (BET) method, and Scanning Electron Microscopy (SEM) analysis. All MIP analyses were done using a UV-Vis spectrophotometer. Binding efficiencies of MIP with domoic acid were determined using batch rebinding experiments, where the optimum mass and time obtained were 5 mg and 15 minutes, respectively. The correlation coefficients (R²) of NIP and MIP were 0.8989 and 0.9933, respectively. The calculated limit of detection (LOD) was 1.418 ppm, and the limit of quantification (LOQ) was 4.2983 ppm. An adsorption isotherm experiment indicated that the Freundlich isotherm model yielded a better fit towards the equilibrium adsorption data. The MIP was successfully applied in the determination of DA in shellfish tissues of cockles and mussels, where the percentage recovery obtained for the spiked samples was 95.88% for cockles and 82.71% for mussels.

Keywords: molecularly imprinted polymer, domoic acid, shellfish, binding efficiency, marine neurotoxin

Abstrak

Polimer tercetak molekul (MIP) domoik asid (DA) telah berjaya disintesis melalui kaedah pempolimeran pukal menggunakan 2-hidroksietil metakrilat (HEMA) sebagai monomer berfungsi dan etilena-glikol dimetakrilat (EGDMA) sebagai penghubung silang. Polimer tidak tercetak (NIP) juga disintesis melalui kaedah yang sama tetapi tanpa penambahan templat molekul (DA). Kehadiran templat DA didalam MIP dan ketidakhadiran templat DA didalam NIP dibuktikan melalui analisis Fourier-Transform Infrared (FT-IR) Spectroskopi, kaedah Bruneaur, Emmett and Teller (BET) dan mikroskopi pengimejan elektron (SEM). Semua MIP dianalisa menggunakan UV-Vis spektrofotometer. Kecekapan pengikatan MIP dengan domoik asid ditentukan melalui ujikaji pengikatan semula secara berkelompok dimana berat dan masa optima yang diperolehi adalah 5 mg dan 15 minit masing-masing. Pekali korelasi (R²) bagi NIP serta MIP adalah 0.8989 dan 0.9933 masing-masing. Pengiraan had pengesanan (LOD) adalah 1.4148 ppm dan had kuantiti (LOQ) adalah 4.2983 ppm. Ujikaji isoterma penjerapan menunjukkan bahawa model isoterma Freudlich menghasilkan data keseimbangan penjerapan yang lebih sesuai. MIP ini telah berjaya diaplikasikan dalam penentuan DA dalam

tisu kerangan iaitu kerang dan kupang dimana nilai peratusan pemulihan yang diperolehi bagi sampel yang dipaku adalah 95.88% bagi kerang dan 82.71% bagi kupang.

Kata kunci: molekul polimer tercetak, domoik asid, kerangan, kecekapan pengikatan, neurotoksin marin

Introduction

Domoic acid (DA) is a type of marine neurotoxin that is responsible for Amnesic Shellfish Poisoning (ASP). It was first documented in 1987, where consumers reportedly fell ill after consuming DA contaminated blue mussels harvested from eastern Prince Edward Island [1]. ASP can cause several illnesses such as diarrhea, degeneration of the nervous system in brain, and short-term memory loss [2]. In the human body, DA is known as an agonist to the glutamate receptor in the brain, where it causes disruption of the flow of mineral ions (Ca, Mg, Zn) across the cell membranes, thus affecting the hippocampus and amygdale glands in the human brain [3]. The DA toxin can be transferred to humans through the food chain via the consumption of toxic microalgae accumulated in seafood [4]. DA bioaccumulation in shellfish is aided by filtration of toxic species of red algae diatom, pseudo-nitzschia [5,6]. The DA molecule (shown in Figure 1), though unstable due to the oxidation of the conjugate double bond, has a strong UV chromophore, marking it as one of the most easily detected toxins [7].

Figure 1. Chemical structure of DA

In order to protect consumers from DA poisoning, i.e., ASP, relevant permitted levels of DA concentration are established by many regulatory authorities, such as in the EU and USA, which is $20~\mu g$ of DA concentration

per gram (g) shellfish meat [8, 9]. The outbreak of DA poisoning in shellfish tissue typically relates to the red tide phenomenon, which occurs during harmful algae blooms [10]. These blooms can be associated with cool and high nutrient water discharge from freshwater reservoirs [11]. Over 52 known species of *Pseudonitzschia* have been recorded globally, and 27 of these species are known to produce DA toxins [12]. In Malaysia, two types of DA producer algae have been recorded: *Nitzschia navis varingica*, which was discovered in peninsular Malaysia [13], and *Pseudonitzschia cuspidata*, which was discovered in Borneo [14].

Researchers have been using many means of analysis to detect DA in seafood. Instruments such as HPLC, GC-MS, and LC-UV are known as the established instruments used for the accurate and precise analysis of DA [15, 16]. However, these methods of analysis are time consuming and expensive. Therefore, in order to provide an alternative sensing method for DA detection, molecular recognition using imprinting polymers is being studied.

Molecularly imprinted polymers (MIPs) are specially designed sorbents that exhibit enhanced selectivity towards a specific structure [17, 18, 19]. They are able to obtain high affinity, robust and stable artificial receptors for the analyte of interest in harsh chemical and physical conditions [20, 21, 22]. The template binds with cross-linkers, monomers, and initiators to produce a set of imprinted memories for the target molecule [23]. The working mechanism of MIPs used in this study is shown in Figure 2. Template molecules (DA), monomer (HEMA), cross-linker (EGDMA), initiator (BPO), and solvent (DMSO) were used for the synthesis of MIPs.

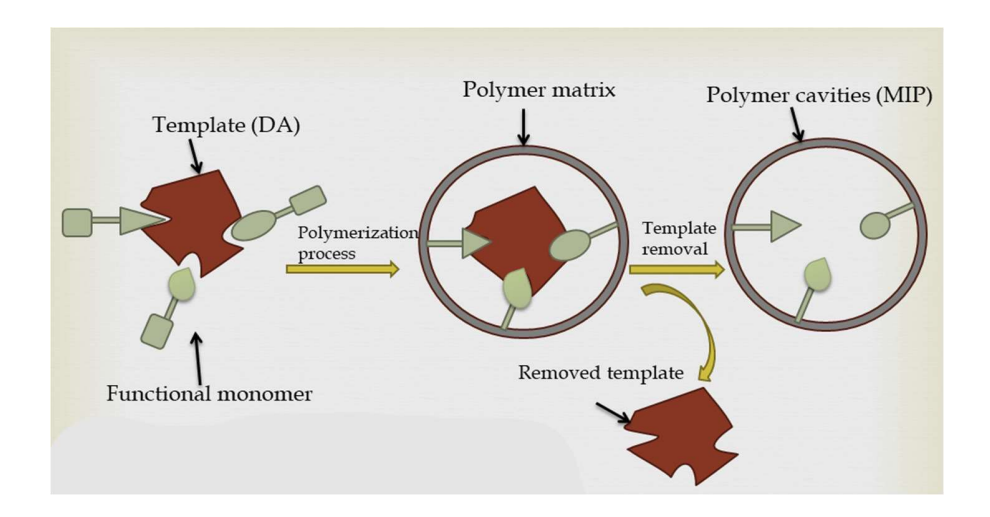


Figure 2. The schematic diagram for the working mechanism of MIP

The pre-polymerized solution was refrigerated for 1 hour in order to slow down the interaction between existing compounds in the solution with oxygen [24]. The polymerization of the MIP was conducted under low temperature conditions ranging from 40°C to 60°C. The cavities were formed by a washing method where the MIP was immersed in methanol/acetic acid (9:1, v/v) to remove the template (DA) [25]. The cavities provide a set of imprinted morphologies and memories capable of selectively binding the template. The imprinted polymer formed after template removal was used in this study to determine the adsorption capacity of MIP with DA.

Materials and Methods

Chemicals and samples

Domoic acid (DA), ethylene glycol dimethacrylate (EGDMA, 98%), hydroxyethyl methacrylate (HEMA, 98%), and benzoyl peroxide (BPO) were purchased from Merck. All other chemicals used in polymer synthesis including acetic acid, methanol, dimethyl sulfoxide (DMSO), and acetone were all analytical grade, and were purchased from Sigma Aldrich. Shellfish samples (cockle and mussel) were purchased from local fishermen and grocery stores.

Instrumentation

The characterization of MIPs and NIPs was conducted using Scanning electron microscopy (SEM), Fourier Transform Infrared (FTIR) spectrometry, and Brunauer,

Emmett, and Teller (BET) Analysis. Meanwhile, the DA detection analysis was performed using Ultraviolet-Visible (UV-VIS) Spectrophotometer.

Synthesis of molecularly imprinted polymers

DA MIP was synthesized by a non-covalent bulk polymerization method. 313.3 µL DA template molecule and 520 µL of monomer (HEMA, 98%) were added into a beaker containing 4.9ml of DMSO. The solution mixture was allowed to stand for 5 minutes. Then, 3.96 mL of cross linker (EDGMA, 98%) was added into the solution, followed by 0.20g of benzoyl peroxide, to initiate the polymerization process. The solution was sonicated for 20 minutes and cooled at -20°C for 1 hour. Then, the polymerization process of MIP was allowed to occur at 40 °C - 60°C for 24 hours using a water bath. The polymers obtained were then filtered and dried for 6 hours at 50°C in an oven. Meanwhile, NIP was synthesized with the same procedure as MIP, but without the addition of a template molecule.

Removal of DA template molecule from MIP

A template removal process was conducted to remove the imprinted DA molecule from the polymer matrix. A successive immersion technique was implemented for the removal of the template. The imprinted polymer was immersed in methanol/acetic acid (9:1, v/v) and shaken using an orbital shaker at 160 RPM for 24 hours at room temperature. The supernatant was filtered and analyzed

to confirm the removal of DA from the MIP. The template removal procedure was conducted until no DA was present in the collected supernatant. The MIP powder was then washed with methanol to remove excess acetic acid. Lastly, the polymer particles were washed with distilled water to remove the remaining solvents. The end product was dried in an oven at 50°C for 6 hours.

Characterization of MIP and NIP

MIPs and NIPs were characterized before and after the template (DA) removal. Morphology and physical characterization studies were carried out using Scanning electron microscopy (SEM), Fourier Transform Infrared (FTIR) spectrometry, and Brunauer, Emmett, and Teller (BET) Analysis.

Batch rebinding experiment

Batch rebinding experiments were conducted to evaluate the performance of MIP binding capacity with DA. Mass and reaction time data was collected using UV-VIS spectrophotometer analysis. The data was analyzed using the Langmuir and Freudlich isotherm model in order to determine the heterogeneity and binding affinity of the MIP with DA.

Reproducibility and Reusability of MIP

Three batches of synthesized MIP were analyzed for their reproducibility by testing their responses with DA analyte for five times. The reusability of MIP was also tested by measuring several detection responses of DA analyte with the same MIP. This involved the repeated processes of reacting, re-washing, and re-reacting MIPs with DA analyte for five reusability cycles. The absorptivity of DA was measured and recorded, and the percentages of relative standard deviations (%RSD) were calculated for the reproducibility and reusability performance of MIP.

Analysis of real samples

The 20g of shellfish tissue and viscera was blended in 25 mL of distilled water and extracted by immersing 10 mL of pureed shellfish samples with 40 ml of methanol/distilled water (1:1; v/v) in a centrifuge tube.

The sample mixture was shaken with a vortex and filtered using a filter paper. The remaining filtered mussel puree was removed and the supernatant collected was labeled as shellfish samples. Spiked and non-spiked samples were prepared by injecting 5ppm of DA for the spiked samples. The spiked and non-spiked shellfish samples were poured into clean vials, labeled, and refrigerated for storage at 4-5°C for further use.

Results and Discussion

Synthesis of MIP and NIP

The MIP and NIP were successfully synthesized through a non-covalent approach using the bulk polymerization method. The functional monomer, HEMA was used in the polymerization process for its neutral functionality, stability, and resistant bond strength [26]. Previous research by Ceolin et al. [27] has proven that the highest imprinting factor for MIPs can be achieved by using the molar ratio of 1:3.5:19.5 for templates, monomers, and cross-linkers. The MIP was synthesized using a 1:4:20 molar ratio of DA template to HEMA monomer to EGDMA cross-linker to provide an MIP with the highest affinity sites, higher selectivity, and adsorption capacity towards analogous compounds [28]. According to Cormack, the ratio of 1:4 of template to functional monomer is commonly used in non-covalent polymerization in favor of the template for the formation of imprinted binding sites. Large amounts of functional monomer will influence the adsorption effect and pore volume of the MIP. Additionally, the molar ratio of template to cross linker (EGDMA) used in the polymerization process is 1 to 20. The polymer to crosslinkers ratio in excess of 80% is often used in the polymerization method. The amount of EGDMA in MIP was studied by Zhao et al., proving the significant effect of cross-linkers dosage on the recognition and adsorption ability of the imprinted polymers. A low amount of EGDMA will cause poor stability and deformation of the polymer cavity, wherein, a high amount of EGDMA will affect the removal process of the template molecule. The polymerization process of MIP was initiated with the presence of BPO in DMSO. The final product obtained was in the form of white powder for both NIP and MIP [29, 30].

Characterization of MIP and NIP: Scanning electron microscopy

The structure and surface morphology of MIP and NIP were observed by using a Scanning Electron Microscope

(SEM) at a magnification of 1000x. The NIP and MIP were synthesized in the form of white powder. The SEM micrographs for MIP and NIP are shown in Figure 3.

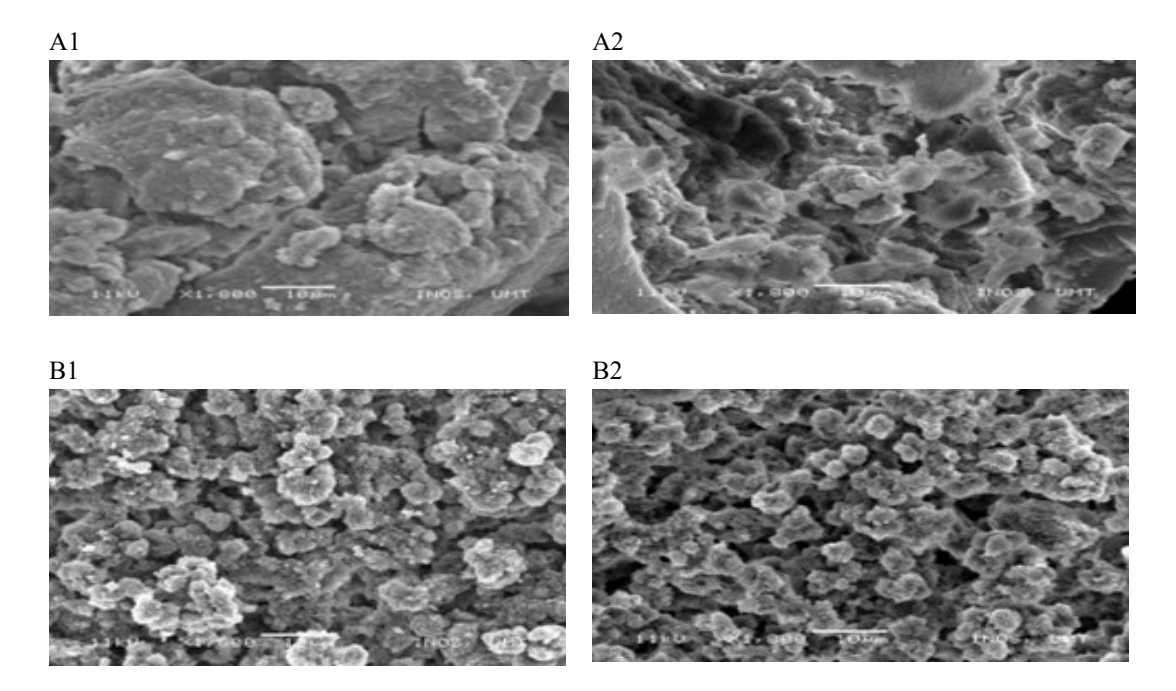


Figure 3. The morphology of MIP and NIP under SEM. A1 and A2 indicates the NIP before and after template removal. Meanwhile, B1 and B2 refer to the MIP before and after template removal

The NIPs before and after the template removal process (A1, A2) exhibit clean surface characteristics with no distinctive pores. The NIP was synthesized without the presence of a template (DA). The NIP after template removal (A2) shows a rougher surface characteristic, which was caused by the removal of unreactive substances from the polymer.

The MIP-DA complex can be seen in Figure 3 (B1 and B2). The pore diameter in B2 is clearer and more prominent when compared to B1. These pores in MIP are the cavities used for embedding the DA template molecule. After the template removal process, the MIP surface was cleaner as all the unreactive particles were flushed from the imprinted polymer, showing complex binding sites and a more distinctive shape than NIP. This difference may be caused by the stable interaction between DA and monomer, where the template was

successfully imprinted onto the polymers during the prepolymerization process. From Figure B1 and B2, it can be seen that both prepared polymer particles are nonspherical and not completely in uniform size and shape, as well as aggregation. This might be caused by the structure of monomer (HEMA) which is quite complicated and has a branched hydrocarbon tail when compared to other monomers such as methacrylic acid (MAA). Therefore, a homogenous spherical shape was unable to be maintained for both MIP and NIP. Another possible reason might due to the inconstant temperature setting (40 °C - 60°C) utilized in the polymerization process. According to Mayes and Whitcombe (2005) [31], the polymerization temperature should be controlled to stabilize the interactions between template and monomer. Low polymerization temperature and low polarity solvents will favor the hydrogen bonding interactions.

Fourier transform infrared

The NIP, MIP-DA, and leached MIP were analyzed under FT-IR spectroscopy as shown in Figure 4. A wide OH stretch can be seen at 3471.68 cm⁻¹, which might indicate the presence of carboxylic acid from the ester group. The presence of imine group (-NH) can be seen at the wavenumber 3408.22 cm⁻¹, where a weak stretch in MIP-DA and MIP spectra exists. The intensity of the NH stretch in MIP is lower than MIP-DA; this might be due to the lack of DA presence in MIP after template leaching. The peak of sp³ CH can be seen at 2954.95 cm⁻ ¹. The intensity of the sp3 CH stretch is almost similar for NIP and MIP-DA, while MIP shows a decrease in the peak intensity. The decrease of peak intensity in the leached MIP might indicate the successful removal of unreacted particles in polymers. At 1720.50 cm⁻¹, a peak of C=O stretching can be seen, with NIP and MIP-DA spectra exhibiting the highest intensity value, albeit MIP-DA spectra showing a slight decrease in intensity,

due to the ester groups of EGDMA [32]. The decrease in intensity of C=O in MIP-DA might be due to the reaction of the cross-linker and DA in the polymer matrix. The low intensity of C=O functional group in MIP might be due to the successful removal of the template (DA). A peak of N-H bend at 1581.63 cm⁻¹ can be seen in MIP-DA and MIP spectra, indicating the presence of DA in the imprinted polymer. The O-H bend of carboxylic acid was exhibited at 1444.68 cm⁻¹ which can be seen present in all spectra. The presence of OH functional group denotes the esters of monomer and cross linkers in the polymer matrix. The stretching of C-O functional group was exhibited by all the spectra at 1188.15 cm⁻¹ and 1139.93 cm⁻¹. The C-O peak of MIP shows a lower intensity than NIP and MIP-DA, as the unreactive particles were removed from the polymer during the leaching process. The sp2 CH bend of alkene can be seen at 991.34 cm⁻¹ in the spectra of NIP, MIP-DA, and MIP.

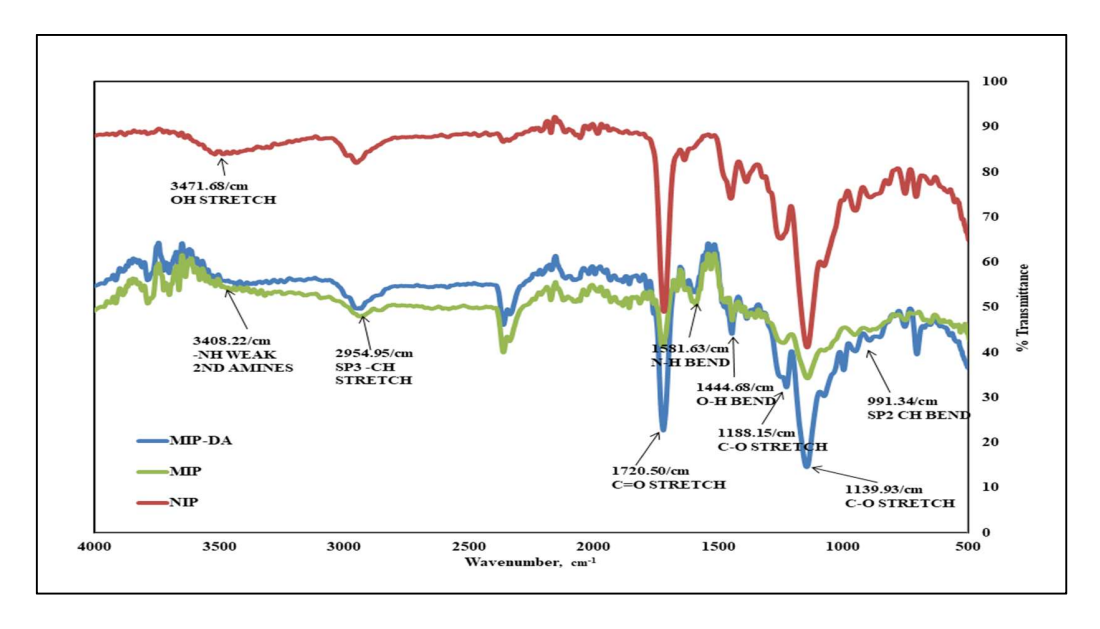


Figure 4. Infrared spectra of Non-Imprinted Polymer, NIP, Molecular Imprinted Polymer, MIP-DA, and MIP after template removal

BET porosity analysis

Figure 5 shows the adsorption-desorption isotherm analysis for NIP, MIP-DA, and MIP polymer matrix. The physisorption isotherm of all polymer matrices exhibits a type IV isotherm. Type IV isotherm is a monolayer-multilayer adsorption and capillary

condensation with complete pore filling. The result indicates that the polymer matrix is mesoporous, with pores in the range of 1.5-100 nm. The type IV isotherm can be characterized by capillary condensation which occurs in mesoporous polymer structures that exhibit a hysteresis loop. In Figure 5 (A), the NIP exhibits H4

type, where polymer contains narrow slit pores including the pores in the micropores region, which conclude that no existing imprint is present in the NIP polymer matrix [33]. Figure 5 (B) and 5(C) prove that MIP was included in the H3 hysteresis type, indicating that the imprinted polymer structure is a non-rigid aggregate with slit shaped 'ink-bottled' pores [34]. Figure 5(C) shows a slightly wider adsorption and desorption region, which indicates an increase in the pore size of MIP after the template removal process. This can be further proven by Table 1, where the pore size of MIP before and after template removal is 11.7nm

and 12.9nm respectively. The surface area and pore volume of NIP is $102 \text{ m}^2/\text{g}$ and $0.29 \text{ cm}^3/\text{g}$ respectively as shown in Table 1, which is smaller than MIP (a) and MIP (b). The result indicates that almost no imprint exists in NIP.

The resulting pore size of NIP might be due to swelling of non-rigid pores in the polymer matrix during the condensation process. The pore size of NIP, MIP(a), and MIP(b) is in the range of 0-100 nm, which verifies that the polymers are mesoporous.

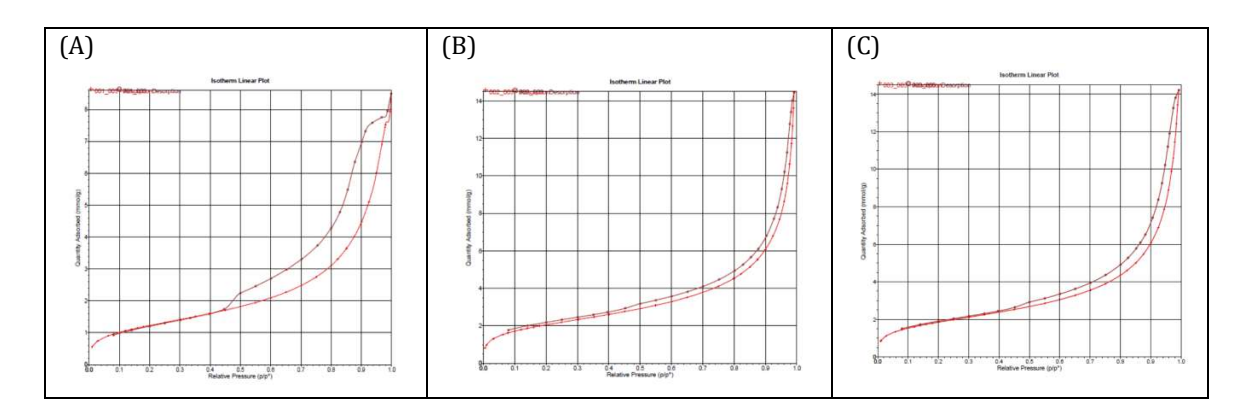


Figure 5. BET adsorption-desorption isotherm analysis of NIP (A), MIP-DA (B), and MIP after DA removal (C). Quantity adsorbed (mmol/g) versus relative pressure (p/p°)

Table 1. Analysis of MIP and NIP porosity using BET

Sample	Surface Area (m²/g)	Area Volume	
NIP	102	0.29	11.5
MIP a	170	0.50	11.7
MIP b	153	0.49	12.9

a: before template removal, b: after template removal

Validation study of DA standard solution

The standard solution of DA was validated using a UV-VIS spectrophotometer at wavelength of 242nm. The validation study was conducted for DA of various concentrations in distilled water. The absorbance value of domoic acid was used to construct a calibration plot as shown in Figure 6. The increasing absorbance value

was clearly shown with increasing DA concentration. The regression correlation for the calibration curve is R²=0.9888 with a slope value of 0.051. The limit of detection (LOD) and limit of quantification (LOQ) for DA was calculated using the formula,

$$LOD = \frac{3.3\sigma}{S} \tag{1}$$

$$LOQ = \frac{10\sigma}{S}$$
 (2)

Where σ refers to the standard deviation of the response and S is the slope value from the calibration curve. The LOD and LOQ values calculated for DA using the formulas are 1.418 and 4.2983 ppm, respectively.

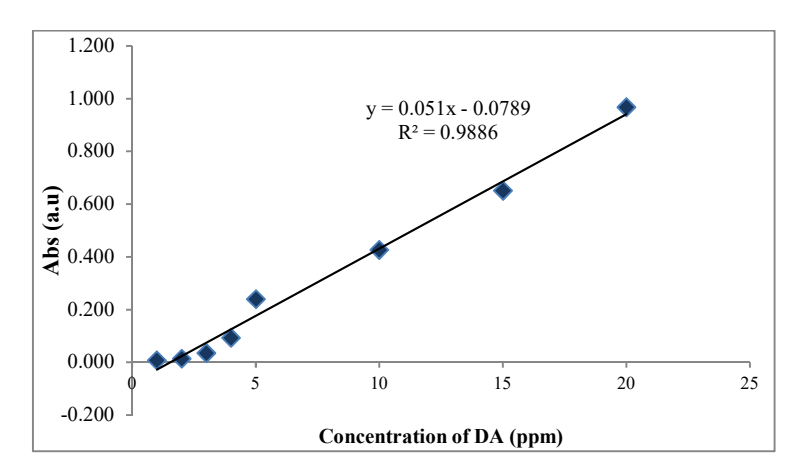


Figure 6. Calibration plot of absorbance (a.u) against concentration of DA (ppm)

Batch rebinding experiments: Adsorption capacity of DA with MIP

The effect of immersion time and mass of molecularly imprinted polymer over domoic acid adsorption capacity was investigated for optimization purposes. Figure 7 shows the graph of adsorption capacity, Qe against immersion time of different masses of MIP with DA at fixed concentration. The binding capacity of MIP was calculated using formula 3.

$$Q_c = \frac{(c_i - c_f)V}{m} \tag{3}$$

Where Q is the adsorption capacity (mg/g), C_i and C_f indicate the initial and final concentrations of DA (ppm), V is the volume of the aqueous solution (ml), and m is the weight of the polymer (g).

The increasing trend of adsorption capacity (Q_e) values for MIP against time in different imprinted polymer weights from zero to fifteen minutes is shown. From 15 to 25 minutes of reaction time, no significant difference in Q_e values can be seen, indicating that the equilibrium concentration of DA in the system was achieved.

Meanwhile, the increasing mass of imprinted polymer shows a significant decrease in Q_e values of the MIP-DA reaction. In Figure 7, 5mg of MIP shows the highest adsorption value when compared to other masses of MIP

used in the study, with a significantly large Q_e value. Low adsorption capacity shown in 10mg, 15mg, 20mg and 25mg of MIP was contributed by deep imprinted pores that cause the bleeding of excess templates in molecular imprinted polymer, resulting in the collapse of the equilibrium system [35]. The equilibrium adsorption capacity for MIP was achieved with the best reaction time and mass of MIP at 15min and 5mg, respectively. The optimum weight and reaction time obtained were 5mg and 15min, respectively.

Reaction response of DA with NIP and MIP

The study for reaction response of NIP and MIP with different concentrations of DA was conducted to determine the selectivity of the sensing system at equilibrium condition as shown in Figure 8 below. The adsorption capacity of DA from a concentration of 1 to 20 ppm shows increasing values for both MIP and NIP. The positive value of adsorption capacity for MIP shows an increasing trend from 1ppm to 20ppm. However, the Qe value for MIP is not significantly large. The results might be due to the low imprinting effect of the MIP where weak imprinted complexes are formed due to the dominant role of the cross-linker during the prepolymerization process [36]. The adsorption capacity of NIP during the adsorption study shows positive results

starting from 10ppm to 20ppm, which indicates the presence of non-selective binding sites on the surface of the polymer. This might be due to the swelling of

polymer surface and the hydrogen bonding interaction between the COOH functional group of DA and the acidic non-specific binding sites of NIP [37].

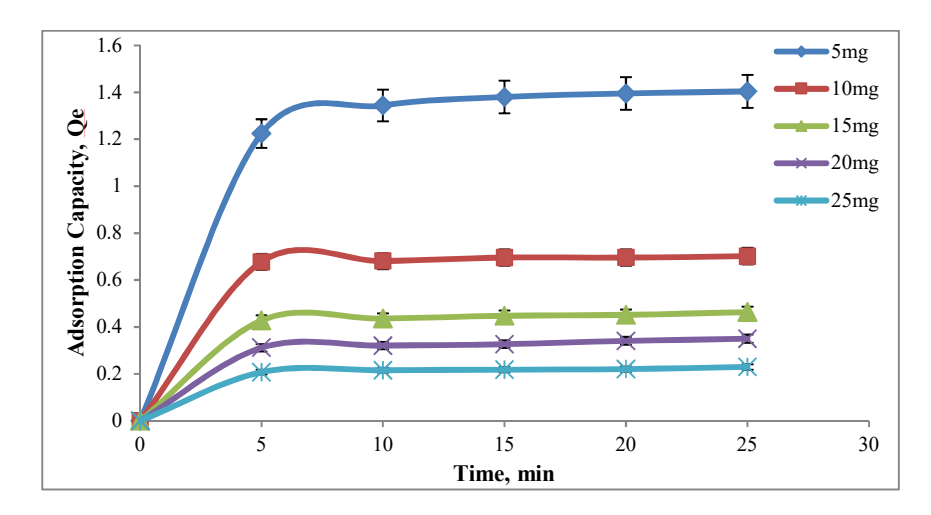


Figure 7. Optimization study of MIP with mass and time as the parameter

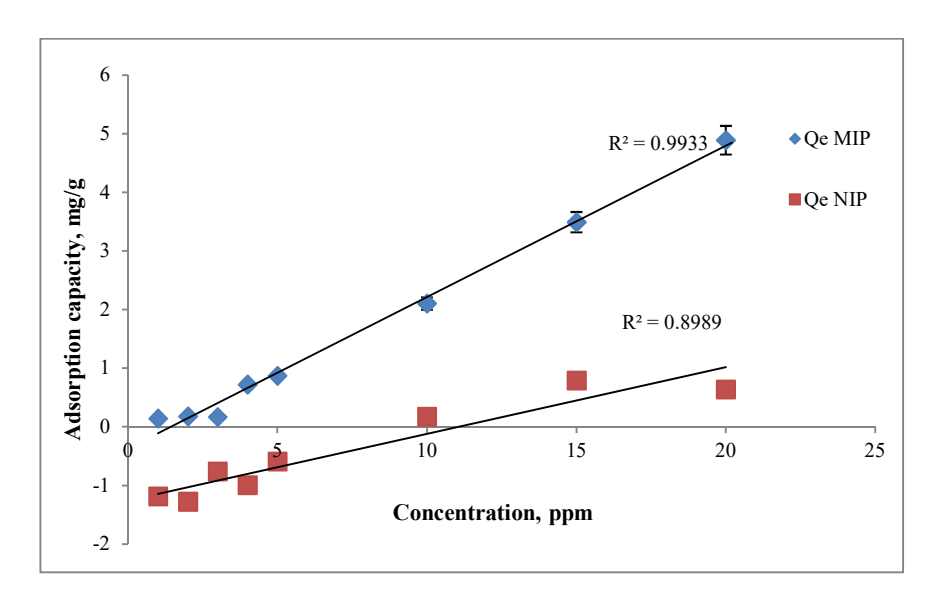


Figure 8. The adsorption capacity of NIP and MIP with various concentrations of DA in equilibrium condition

Adsorption isotherm study

Adsorption isotherm is described as the retention (release) of substances on a solid in various concentrations [38]. The Langmuir isotherm is defined as a system where homogenous adsorption of fixed, localized, identical sites project similar affinities to adsorbate, where no further reaction occurs approaching

equilibrium saturation point [39]. The model can be linearized and non-linearized according to the formulas 4 and 5 shown below.

$$Qe = \frac{Q_O K_L C_e}{1 + K_L C_e} \tag{4}$$

$$\frac{1}{Q_e} = \left(\frac{1}{Q_O K_L}\right) \frac{1}{C_e} + \frac{1}{Q_O} \tag{5}$$

Where Q_e indicates the binding capacities at equilibrium (mg/g); Q_o denotes the maximum adsorption capacities of the adsorbate (mg/g); K_L refers to the Langmuir constant (L/mg); C_e is the concentration of domoic acid at equilibrium (ppm). The data was fitted into a Langmuir isotherm model of $1/C_e$ versus $1/Q_e$ as plotted in Figure 9(a). The separation factor, R_L of the Langmuir isotherm was calculated using formula 6.

$$R_L = \frac{1}{1 + K_L C_O} \tag{6}$$

Where K_L indicates the Langmuir constant (L/mg) and C_O refers to the initial concentration of DA (ppm).

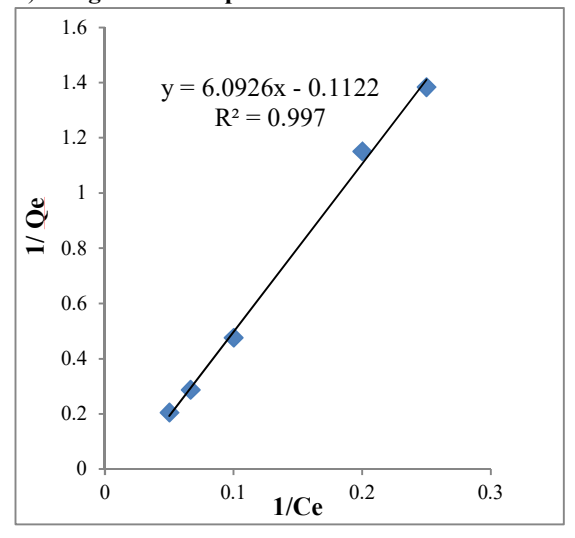
The Freundlich isotherm model is used to analyze the adsorption isotherm in order to define the surface heterogeneity and adsorption intensity of the adsorbate sites. The linear and non-linear equations of the model were indicated as shown in formula 7 and 8, respectively.

$$Q_e = K_f C_e^{\frac{1}{n}} \tag{7}$$

$$log Q_e = log K_f + \frac{1}{n} log C_e$$
 (8)

Where K_f indicates the adsorption capacity (L/mg) and 1/n refers to the adsorption intensity. This isotherm model was fitted into a graph by plotting log C_e against log Q_e as shown in Figure 9(b).

a) Langmuir adsorption isotherm



b) Freundlich adsorption isotherm

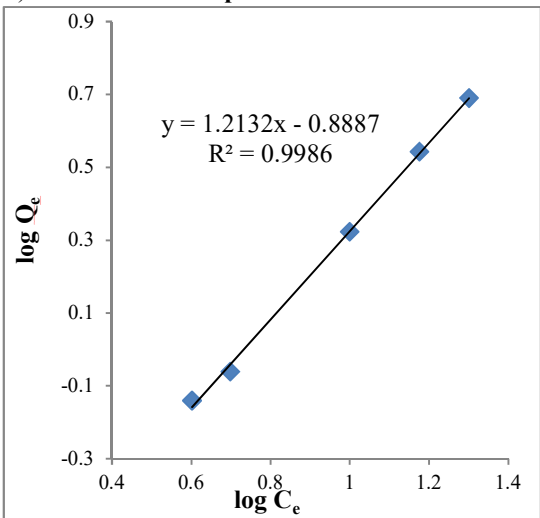


Figure 9. The graph of adsorption isotherm model study of MIP with DA where; a) Langmuir adsorption isotherm, b) Freundlich adsorption isotherm

The separation factor (R_L) value was used to conclude the favorability of adsorption. R_L values more than 1 indicate that an unfavorable adsorption occurs in the system. Linear adsorption occurs when $R_L=1$, while irreversible adsorption occurs when $R_L=0$. However, $0 < R_L < 1$ indicates favorable adsorption [40]. From table 2, the R_L values for the Langmuir isotherm were calculated, where $R_L>1$. It indicates unfavorable

adsorption reactions occurring in the environment. The value of K_L is less than zero, which implies that a large surface area and pore volume of MIP results in a lower adsorption capacity [41].

The experimental data was fitted into the Freundlich isotherm model in order to define the surface heterogeneity and adsorption intensity of the adsorbate

sites. Meanwhile, for the Freundlich isotherm model, the value of 1/n that represents the adsorption intensity is more than 1, indicating cooperative adsorption between DA and MIP.

The R² of the Freundlich model is 0.9986 which is approaching 1 compared to the Langmuir model where

the R^2 is 0.997. From R^2 values, the Freundlich model isotherm is better fitted for DA and MIP binding systems rather than the Langmuir isotherm model. The result suggests that multilayer chemisorption occurs for DA in MIP [42]. The calculated data for parameters representing the Langmuir and Freundlich isotherm models is tabulated in Table 2.

Table 2. Constant	narameters of I	anomiiir a	ind Freundlic	h Isotherm	model for MIP
radic 2. Constant		Jangman a	ma i reamanc		

Isotherm Model	Langmuir	Freundlich
Equation	y = 6.0936x - 0.1122	y=1.2132x-0.8887
$Q_o (mg/g)$	-8.9126	-
$K_L \left(L/mg \right)$	-0.0184	-
$R_{ m L}$	1.1013	-
1/n	-	1.2132
n	-	0.8243
$K_{\rm f}\left(mg/g\right)$	-	0.4112
\mathbb{R}^2	0.997	0.9986

Reproducibility of MIP

This study was conducted to analyze the effectiveness and practicability of the preparation method and whether it can be reproduced in its entirety under changing conditions [43]. Five batches of MIP were synthesized in triplicates under optimized conditions. The data collected was analyzed, and a graph was constructed (as

shown in Figure 10) to exhibit the reproducibility of the MIP sensing system. The five (5) batches of MIP showed no significant difference in absorbance values. The %RSD for the reproducibility of MIP was calculated, with the value ranging from 3.22% - 5.19% (n=5). The low values of %RSD reflect the good performances of MIP in DA determination.

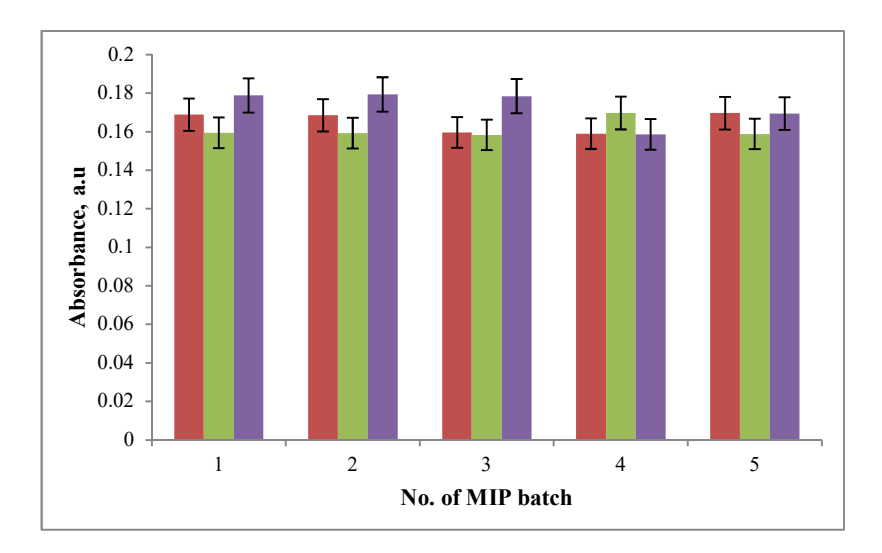


Figure 10. The reproducibility study of MIP in optimized condition

Reusability of MIP

Reusability is defined as repeat measurements made on the same subject under identical conditions. The reusability study was conducted by using one (1) set of MIP for five cycles of DA adsorption. The MIP was rewashed and re-used to reflect the reusability of the sensing system. The absorbance values for each cycle in the reusability analysis are shown in Figure 11. From Figure 11, cycles 1 to 3 show no difference in absorbance values, indicating the stability in DA detection. However, the fourth cycle shows a high value of DA present in the system. This condition might occur due to the bleeding of un-leached template molecules that are retained in the MIP from the first three cycles. The %RSD value calculated for the reusability test is 2.97% (n=5), which indicates the suitability of MIP as a disposable sensor for the detection of DA, which can be used three times.

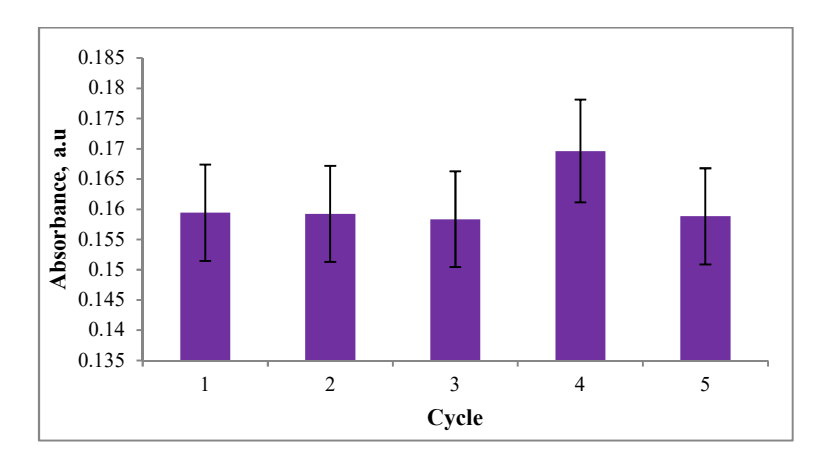


Figure 11. The reusability of MIP for adsorption of DA in 5 cycles

Application of MIP with real samples

The selected shellfish (cockle and mussel) used for this study were purchased from local fishermen and grocery stores. Table 3 shows the final concentration and percentage recovery for spiked and non-spiked cockle and mussel samples.

Table 3. Spike and recovery results of domoic acid in cockle and mussel tissue

Types of	Non-	Spiked (5 ppm)		
Shellfish	spiked	Final Concentration,	%	
		ppm	Recovery	
Cockle	Undetected	4.79	95.88	
Mussel	Undetected	4.13	82.71	

From the initial concentration (5ppm) of DA used, 4.79ppm and 4.13ppm were recovered from the spiked tissue of cockle and mussel, respectively, using the MIP sensing system. The percentage recovery for cockle and mussel was calculated to be 95.88% and 82.71%, respectively. However, no DA was presence was detected from non-spiked samples when analyzed using UV-VIS spectrophotometry.

Conclusion

In this study, a selective and sensitive MIP sensing system was successfully synthesized using non-covalent bulk polymerization techniques. The lower values of %RSD for reproducibility and reusability of MIP indicate better performances for the sensing system. From the adsorption isotherm analysis, the Freudlich isotherm model was found to be a better fit for analyzing the binding affinity of MIP with DA. The MIP sensing

system for DA was successfully applied to real samples (cockle and mussel).

Acknowledgement

The authors would like to acknowledge the Ministry of Education Malaysia through Fundamental Research Grant Scheme of FRGS/1/2015/ST04/UMT/02/1 (FRGS 59409) and Universiti Malaysia Terengganu for providing support, laboratory facilities, and instrumentation.

References

- Maeno, Y., Kotaki. Y., Terada. R., Cho. Y., Konoki. K. and Yamashita M.Y. (2018). Six domoic acid related compounds from the red alga, chondria armata, and domoic acid biosynthesis by the diatom, Pseudo-Nitzschia Multiseries. Scientific Reports, 8: 356.
- 2. Costa, L. G., Giordano. G. and Faustman. E. M. (2010). Domoic acid as a developmental neurotoxin. *Neurotoxicology*, 31(5): 409-423.
- 3. Pulido, O. M. (2008). Domoic acid toxicologic pathology: A review. *Marine Drugs*, 6(2): 180-219.
- Zaelinski, O., Busch, J. A., Cembella, A. D., Daly, K. I., Engelbrektsson, J., Hannides, A. K. and Schmidt, H. (2009). Detecting marine hazardous substances and organisms: sensors for pollutants, toxins and pathogens. *Ocean Science*. 5: 329-349.
- Costa, P. R., Rosa, R., Duarte-Silva, A., Brotas, V. and Sampayo, M. A. M. (2005). Accumulation, transformation and tissue distribution of domoic acid, the amnesic shellfish poisoning toxin, in the common cuttlefish, sepia officinalis. *Aquatic Toxicology*, 74: 82-91.
- Ayache, N., Fabienne. H., Veronique. M-J., Amzil. Z. and Amandine. M. N. C. (2019). Influence of sudden salinity variation on the physiology and domoic acid production by two strains of *pseudo*nitschia australis. Journal of Phycology, 55(1): 186-195.
- Kreuzer, M. P., Pravda, M., O'Sullivan, C. K. and Guilbault, G. G. (2002). Novel electrochemical immunosensors for seafood toxin analysis. *Toxicon*, 40: 1267-1274.

- 8. Hortigüela, M. J. and Wall, J. G. (2013). Improved detection of domoic acid using covalently immobilised antibody fragments. *Marine Drugs*, 11: 881-895.
- Mohd Syaifudin, A. R., Jayasundera, K. P. and Mukhopadhyay, S. C. (2009). A low-cost novel sensing system for detection of dangerous marine biotoxins in seafood. *Sensors and Actuators B*, 137: 67-65.
- Mohd Syaifudin, A. R., Jayasudera, K. P. and Mukhopadhyay, S.C. (2008). Initial investigation of using planar interdigital sensors for assessment of quality in seafood. *Journal of Sensors*, 2008: 1-9.
- Busse, L. B., Venrick, E. L., Antrobus, R., Miller, P. E., Vigilant, V., Silver, M. W., Mengelt, C. and Mydlarz, L. and Prezelin, B. B. (2006). Domoic acid in phytoplankton and fish in San Diego, CA, USA. *Harmful Algae*, 5 (2006): 91-101.
- Bates, S. S., Hubbard, K. A., Lundholm, N., Montresor, M. and Leaw, P. C. (2018). *Pseudo-nitzschia*, *Nitzschia*, and domoic acid: New research since 2011. *Harmful Algae*, 79:43.
- Tan, S. N., Teng, S. T., Lim, H. C., Kotakid, Y., Bates, S. S., Leaw, C. P. and Lima, P. T. (2016).
 Diatom Nitzschia Navis-Varingica (Bacillariophyceae) and its domoic acid production from the mangrove environments of Malaysia. Harmful Algae, 60: 139-149.
- 14. Teng, S. T., Abdullah, N., Hanifah, A. H., Tan, S. N., Gao, C., Law, I. K., Leaw, C. P and Lim, P. T. (2021). Toxic bloom of Pseudo-nitzschia cuspidata (Bacillariophyceae) and domoic acid contamination of bivalve molluscs in Malaysia Borneo. Toxicon, 202: 132-141.
- Mitcheli, L., Radoi, A., Guarrina, R., Massaud, R., Bala, C., Moscone, D. and Palleschi, G. (2004). Disposable immunosensor for the determination of domoic acid in shellfish. *Biosensors and Bioelectronics*. 20: 190-196.
- Barbaro, E., Zangrando, R., Barbante, C and Gambaro, A. (2016). Fast and sensitive method for determination of domoic acid in mussel tissue. *The Scientific World Journal*, 2016: 1-6.

- 17. Tom, L. A., Schneck, N. A. and Walter, C. (2012). Improving the imprinting effect by optimizing template:monomer:cross-linker ratios in a molecularly imprinted polymer for sulfadimethoxine. *Journal of Chromatography B*, 909(2012):61-64
- Haupt. K., Rangel. P. X. M. and Bui. B. T. S. (2020). Molecularly imprinted polymers: antibody mimics for bioimaging and therapy. *Chemical Reviews*, 120(17): 9554-9582.
- Lopes, F., Pacheco, J. G., Rebelo, P. and Cristina, D. M. (2017). Molecularly imprinted electrochemical sensor prepared on a screen-printed carbon electrode for naloxone detection. Sensors and Actuators B: Chemical, 243 (2017): 745-752.
- Ashley. J., Mohammad-Ali. S., Kant. K., Chidambara. V. A., Wolff. A., Bang. D. D, and Sun. Y. (2017). Molecularly imprinted polymers for sample preparation and biosensing in food analysis: progress and perspectives. *Biosensors and Bioelectronics*, 91(2017): 606-615.
- Beltran, A., Borrull, F., Marcé, R. M. and Cormack,
 P. A. G. (2010). Molecularly-imprinted polymers: useful sorbents for selective extractions. *TrAC Trends in Analytical Chemistry*, 29(11): 1363-1375.
- 22. Zhou, W. H., Guo, X. C., Zhao, H. Q., Wua, S. X., Yang, H. H. and Wang, X. R. (2011). Molecularly imprinted polymer for selective extraction of domoic acid from seafood coupled with high-performance liquid chromatographic determination. *Talanta*, 84(3):777-782.
- 23. Nemoto, K., Kubo, T., Nomachi, M., Sano, T., Matsumoto, T., Hosoya, K., Hattori, T. and Kaya, K. (2007). Simple and effective 3D recognition of domoic acid using a molecularly imprinted polymer. *Journal American Chemical Society*, 129(44): 13626-13632.
- Royani, I., Widayani., Abdullah, M. and Khairurrijal. (2014). Effect of heating time on atrazine-based MIP materials synthesized via the cooling-heating method. *Advanced Materials Research*, 896(2014): 89-94.
- 25. Royani, I., Widayani., Abdullah, M. and Khairurrijal. (2014). An atrazine molecularly imprinted polymer synthesized using a cooling-heating method with repeated washing: its physico-

- chemical characteristics and enhanced cavities. *International Journal Electrochemical Sciences*, 9: 5651-5662.
- Kintopp, C. C. A., Furuse, A. Y., Costa, R. M., Lucena, F. S., Correr, G.M. and Gonzaga, C. C. (2020). Influence of acidic monomer concentration and application mode on the bond strength of experimental adhesives. *Brazilian Oral Research*, 2020(34):105.
- Ceolin, G., Navarro- Villoslada F., Moreno-Bondi, MC., Horvai, G. and Horvath., V. (2009). Accelerated development procedure for molecularly imprinted polymer using membrane filterplates. *Journal of Combinatorial Chemistry*, 11(4): 645-652.
- Hasanah, A. N., Safitri, N., Zulfa, A., Neli, N. and Rahayu. D. (2021). Factors affecting preparation of molecularly imprinted polymer and methods on finding template-monomer interaction as the key of selective properties of the materials. *Molecules*, 26: 5612.
- 29. Cormack, P. A. G. and Elorza, AZ. (2004). Molecularly imprinted polymers: synthesis and characterization. *Journal of Chromatography B*, 804: 174-178.
- Zhao, G., Liu, J., Liu, M., Xiaobin Han, X., Peng, Y., Xiatian Tian, X., Liu., J. and Zhang., S. (2020). Synthesis of molecularly imprinted polymer via emulsion polymerization for application in solanesol separation. *Applied Sciences*, 2020(10): 2868.
- 31. Mayes, A. G. and Whitcombe, M. J. (2005). Synthetic strategies for the generation of molecularly imprinted organic polymers. *Advanced Drug Delivery Reviews*, 57(12): 1742-1778.
- 32. Yang, F., Wang, R., Na, G., Yan, Q., Lin, Z. and Zhang, Z. (2018). Preparation and application of a molecularly imprinted monolith for specific recognition of domoic acid. *Analytical and Bioanalytical Chemistry* 410: 1845-1854.
- Marinah, M. A., Yatim, N. I. and Tahir, N. M. (2015). Selective surface characteristics and extraction performance of a nitro-group explosive molecularly imprinted polymer. *Malaysian Journal of Analytical Sciences*, 19(3): 574-585.

- 34. Zeng, Y., Fan, C., Do, D. D. and Nicholson, D. (2014). Evaporation from an ink-bottle pore: mechanisms of adsorption and desorption. *Industrial Engineering Chemical Research*, 2014(53): 15467-15474.
- 35. Lorenzo, R. A. (2011). To remove or not to remove? the challenge of extracting the template to make the cavities available in molecularly imprinted polymers (MIPs). *Journal Molecular Sciences*, 12(7): 4327-4347.
- 36. Hasanah, A. N., Safitri, N., Zulfa, A., Neli, N. and Rahayu. D. (2021). Factors affecting preparation of molecularly imprinted polymer and methods on finding template-monomer interaction as the key of selective properties of the materials. *Molecules*, 26: 5612.
- Anene, A., Kalfat, R., Chevalier, Y. and Hbaieb, S. (2020). Design of molecularly imprinted polymeric materials: The crucial choice of functional monomers. *HAL Open Science*, 2020(3): 769-781.
- Limousin, G., Gaudet, J. –P., Charlet, L., Szenknect, S., Barthes, V. and Krimissa, M. (2006). Sorption isotherms: a review on physical bases,

- modeling and measurement. *Applied Geochemistry*, 22(2): 249-275.
- 39. Kundu, S. and Gupta, A. K. (2006). Arsenic adsorption onto iron oxide-coated cement (IOCC): Regression analysis of equilibrium data with several isotherm models and their optimization. *Chemical Engineering Journal*, 122(1-2): 93-106.
- 40. Foo, K. Y. and Hameed, B. H. (2010). Insights into the modeling of adsorption isotherm systems *Chemical Engineering Journal*, 156: 2-10.
- 41. Ayawei, N. (2017). Modelling and interpretation of adsorption isotherms. *Hindawi Journal of Chemistry*, 2017:1-17.
- 42. Hande, P. E., Samui, A. B. and Kulkarni, P.S. (2015). A molecularly imprinted polymer with flash column chromatography for the selective and continuous extraction of diphenyl amine. *RSC Advances*, 5: 73434.
- 43. Bartlett, J. W. and Frost, C. (2008). Reliability, repeatability and reproducibility: analysis of measurement errors in continuous variables. *Ultrasound in Obstetrics and Gynecology*, 31(4): 466-475.